Dynamic Study of Crystallization- and Melting-Induced Phase Separation in PEEK/PEKK Blends

Wu Wang[†] **and Jerold M. Schultz***

Materials Science Program, University of Delaware, Newark, Delaware 19711

Benjamin S. Hsiao*[,‡,§]

Central Research and Development, E. I. du Pont de Nemours & Company, Inc., Experimental Station, Wilmington, Delaware 19880

Received January 24, 1997; Revised Manuscript Received May 14, 1997[⊗]

ABSTRACT: Kinetics of lamellar microstructure development of poly(aryl ether ether ketone) (PEEK), poly(aryl ether ketone ketone) containing 70% isophthalate moieties (PEKK(30/70)) and their 50/50 blend during isothermal crystallization and subsequent melting have been studied by DSC, transmitted light intensity, and time-resolved small-angle X-ray scattering (SAXS). The crystallization peak time, spherulite growth rate, and dimensions of lamellar stacks (long period L, crystal lamellar thickness l_c and amorphous layer thickness l_a) were determined. It was found that there is a remarkable difference in the crystallization kinetics of pure PEEK and PEKK(30/70). In the blend, the addition of PEKK(30/70) significantly reduces the crystallization rate of PEEK, resulting in a peak time intermediate between the two neat materials. A two-step behavior was observed during isothermal crystallization and subsequent melting processes in the blend by both transmitted light intensity and time-resolved SAXS techniques. Results show no sign of cocrystallization or epitaxial growth between the crystals of PEEK and PEKK(30/70) rather than the coexistence of two separate lamellar structures (PEEK and PEKK(30/70)) in the same spherulites. It is thus concluded that during crystallization, PEEK spherulites formed first followed by the infilling of PEKK(30/70) crystals within these spherulites.

Introduction

Poly(aryl ether ether ketone) (PEEK) is a well-known high-performance engineering thermoplastic material. It offers excellent chemical resistance and physical and mechanical properties at elevated temperatures. In recent years, it has been broadly used in commercial applications where high temperature and high strength are required.[1−4] Poly(aryl ether ketone ketone)s (PEKKs) constitute a new set of material. Like PEEK, PEKKs also possess high melting temperatures and high glass temperatures,[5,6] and thus can also serve as excellent melt-processible matrix materials for composites. Both PEEK and PEKKs are members of the poly(aryl ether ketone) (PEAK) family and are of high commercial and scientific interest.

Of the two polymers, PEEK has received more attention thus far, and considerable progress has been made in the understanding of its crystalline structure,[7−11] optical and lamellar morphologies,[12−18] crystallization kinetics,[19−21] and physicochemical properties.[22,23] There are significant differences in the reported results of lamellar structure and lamellar stack dimensions of PEEK.[11,16,17] However, it is agreed that the lamellar morphology of PEEK depends on its thermal history, and its long period L and lamellar thickness l_c are functions of crystallization temperature.[11,17] Based on the common observation in PEEK that both L and l_c decrease with time in the early stage of melt crystallization, different models of lamellar evolution, such as the lamellar insertion model[15−17] and dual lamellar stacks model,[12,19,26] have been proposed to explain this finding.

PEKKs are prepared from diphenyl ether (DPE), terephthalic acid (T), and isophthalic acid (I) in a two-stage process. The ratio of T and I can be controlled from 100/0 to 0/100. By incorporating the I moiety into the PEKK crystals, the melting temperature of PEKK can be lowered, and the crystallization behavior can be significantly changed without the reduction of T_g and its end use temperature.[6] Several studies of crystallization behavior,[6,27,28] morphology, and polymorphism[29,30] in PEKKs have been reported. Ho *et al.* found that even though multiple polymorphs can be observed in different crystals as functions of I content and crystallizing conditions, the general morphological appearances of PEKK spherulites are similar to that of PEEK.[29,30] Both materials produce spherulites with narrow, elongated lamellae, that grow radically in the crystallographic b-axis direction.

While there are many similarities between PEEK and PEKKs, remarkable dissimilarities also exist between the two, especially in crystallization kinetics and crystallization behavior. For example, PEEK has a very fast crystallization kinetics while PEKKs offer a broad range of crystallization rate that can be controlled by varying the T/I ratio. It is thus possible to optimize the desired properties by blending the two. Up to now there has been no study of the crystallization behavior in the PEEK and PEKK blends. The object of this work thus is to investigate the crystallization kinetics and lamellar structures of the PEEK/PEKK blends. DSC and transmitted light intensity measurements were used to investigate the kinetics, and time-resolved small-angle X-ray (SAXS) experiments were carried out to study the phase behavior and lamellar evolution. Finally, a model has been proposed to explain the development of lamellar structure in the blend.

---

* To whom all correspondence should be addressed.

[†] Current address: Chemistry Department, Queen's University, Kingston, Ontario, Canada K7L 3N6.

[‡] Tel.: 302-695-4668. Fax: 302-695-1717. E-mail: hsiaobs@esvax.dnet.dupont.com.

[§] Current address: Chemistry Department, State University of New York at Stony Brook, Stony Brook, NY 11794-3400.

[⊗] Abstract published in *Advance ACS Abstracts,* July 1, 1997.

S0024-9297(97)00092-2 CCC: $14.00 © 1997 American Chemical Society

Experimental Section

Materials and Sample Preparation. Commercially available PEEK (Type 150G) from ICI was used in this experiment. It has a T_g of 145 °C and an equilibrium melting temperature $T_m°$ of 395 °C.[1] The weight-average molecular weight M_w and number-average molecular weight M_n are 38 000 and 14 000, respectively. The PEKK used in this study was PEKK(30/70). It contains 30% T and 70% I moieties and was synthesized by Dr. K. L. Faron of DuPont CR&D. This polymer has a M_w of 30 000 and M_n of 10 000.[31] The T_g of PEKK(30/70) is about 153 °C, slightly higher than PEEK's T_g, whereas the $T_m°$ is 303 °C, which is much lower than that of PEEK. In addition, the crystallization kinetics of PEKK(30/70) is much slower than that of PEEK, which makes it ideal for studying the phase behavior of the blends. The mixing was carried out by a lab-size extruder (CSI model 194A). The blending temperature was 390 °C. Only one ratio of the blend (50/50) was used in this study.

Thin film samples (ca. 5 μm) for optical microscopy and transmitted light intensity measurements were prepared by melting the powder material under pressure between a microscope slide and a cover glass at about 10 deg above $T_m°$. For small-angle X-ray scattering (SAXS) experiments, void-free sample disks with dimensions of 6.75 mm in diameter and 1.1 mm in thickness were prepared. All the materials used were vacuum dried at 100 °C for 24 h prior to the sample preparation or measurements.

Characterization Methods. A Perkin-Elmer DSC-7 instrument was utilized to study the isothermal crystallization kinetics. In this experiment, all samples were first equilibrated at 10 deg above $T_m°$ for 3 min to eliminate the residual crystallinity and then rapidly cooled to the desired temperature for measurement. The crystallization peak time was taken at the maximum exothermic heat flow. For PEEK, the crystallization isotherms at low temperatures (<170 °C) were measured using a cold crystallization technique,[11] and no measurement was made between 170 and 300 °C since the crystallization rate in this range is too fast to be accurately determined by our instruments.

A thermal optical analysis (TOA) system was used for optical microscopy and transmitted light intensity measurements under cross polars. The system consists of a Mettler FP82 hot stage, a polarizing optical microscope (Nikon Optiphot-PDL), a VCR, a CCD camera, a Mettler photometer, and a computer. During the experiment, the thin film sample was first melted on a hot plate at 10 deg above $T_m°$ for 3 min and then rapidly transferred to the hot stage (held at the desired temperature) for measurement. Real time images of spherulite growth were recorded by the CCD camera and VCR, and the transmission light intensity was measured by the photometer. The JAVA image analysis program was used to analyze the images to determine the spherulite growth rate.

Synchrotron SAXS experiments were performed at the X3A2 beamline (wavelength 1.54 Å) at the National Synchrotron Light Source, Brookhaven National Laboratory. The SAXS profiles were collected using modified Kratky optics[32] and a linear position-sensitive detector (Braun). A dual-chamber temperature-jump device[33] was used for this measurement. The sample was first melted in the high-temperature chamber ($T_o = T_m° + 10$ °C) for 3 min to reach thermal equilibrium and then was jumped to the low-temperature chamber at a desired crystallization temperature T_c. The cooling rate of the sample from T_o to T_c was about 300 °C/min, and the thermal equilibrium at T_c could be reached between 20 and 60 s. The collected scattering angular range was $2\theta = 0.21-2.81°$. Typical data collection time was selected between 10 and 25 s. All SAXS profiles were corrected for sample absorption, background scattering and incident beam fluctuation. The correlation function $\gamma(r)$ was calculated after further data smoothing and Porod's law fitting at large q range ($q = 4\pi(\sin\theta)/\lambda$). The correlation function is defined as[34]

$$\gamma(r) = \frac{1}{2\pi^2}\int_0^\infty (I(q) - I_b)q^2\cos(qr)\,dq \tag{1}$$

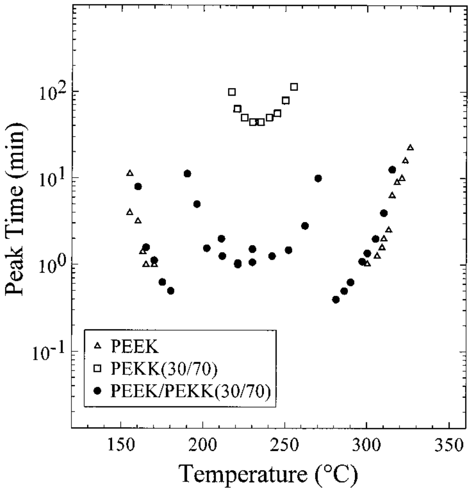

Figure 1. Crystallization peak times of PEEK, PEKK(30/70), and the blend determined by DSC.

where $I(q)$ is the scattering intensity, and I_b is the background intensity, obtained by fitting the tail of SAXS profile to Porod's law. From the correlation function, we estimate the long period of the lamellar structure L (the first maximum), crystal lamellar thickness l_c, and thickness of the interlamellar amorphous region l_a using the following equations (assuming a two-phase morphology)[35]

$$x_{cl}(1 - x_c)L = B$$
$$x_{cl} = l_c/L$$
$$l_a = L - l_c \tag{2}$$

where $x_{cl} = l_c/L$ is the linear crystallinity within the lamellae structure and B is the position of the first zero of the correlation profile.

There are two kinds of long period, L_B and L_c^M, that can be extracted from SAXS profiles. L_B represents the long period calculated by applying Bragg's law to the maximum in the Lorentz plots, and L_c^M is the long period estimated from the correlation function (the first maximum). As pointed out by other authors,[11] L_B is usually greater than L_c^M. The difference between L_B and L_c^M is normally between 5% and 20% and is caused by some combination of the following factors: deviation of the real structure from the ideal two-phase model, errors introduced during the data collecting process and the data treatment, and the calculation of the correlation function. The difference between L_B and L_c^M in the present study is about 7%, and both show similar trends. L_c^M is denoted as L hereafter in this paper.

Results and Discussion

DSC Measurements. Figure 1 illustrates results of crystallization peak time versus crystallization temperature T_c for PEEK, PEKK(30/70), and the blend. It is seen that within the temperature range studied, PEEK has much shorter peak times (about 3 orders of magnitude), i.e., faster crystallization rates, than PEKK(30/70). Both maximum crystallization rates of PEEK and PEKK(30/70) occur near 240 °C, but it shifts slightly to a lower temperature (~220 °C) for the blend. At both high (≥280 °C) and low (≤180 °C) temperature regions, the crystallization rate of the blend closely tracks that of PEEK. We believe this is because the crystallization rate of PEKK(30/70) is too slow in these regions and the measured exotherm is mainly due to PEEK. As the temperature approaches the maximum rate region (180 °C < T < 280 °C), the peak time of the blend becomes intermediate between the two neat polymers. At some temperatures, two exothermic peaks can be seen in the

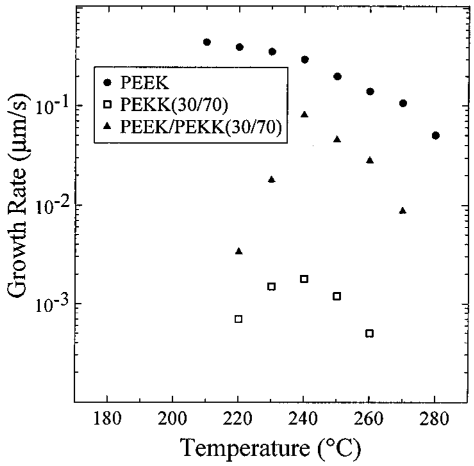

Figure 2. Spherulite growth rates of PEEK, PEKK(30/70), and the blend determined by TOA.

DSC isothermal scans. The change from the PEEK tracking behavior to the intermediate response is very abrupt near the two transition temperatures (180 and 280 °C). In this study, we have limited our focus to the crystallization behavior in the region between these two temperatures.

Figure 2 shows spherulite growth rates of the neat materials and the blend by optical microscopy at temperatures between 180 and 280 °C. Typically, three to four separate measurements were made to obtain the average growth rate with good statistics. In this figure, it is seen that the growth rate of the blend lies between those of the neat materials, which is similar to the behavior in Figure 1. One important observation here is that we did not find two spherulite morphologies in the blend. This indicates that only one kind of spherulite exists in the blend and both neat crystals coexist within these spherulites.

Transmitted Light Intensity Measurements. Parts a–c of Figure 3 show profiles of transmitted polarized light intensity versus time during isothermal crystallization of PEEK, PEKK(30/70), and the blend. This transmitted intensity is proportional to the amount of the materials crystallized. Since PEEK has a faster growth rate, its transmitted intensities reach plateau values all within very short times (Figure 3a, a few minutes or less, which are consistent with DSC results in Figure 1). In contrast, the measured intensities of PEKK 30/70 are considerably longer (Figure 3b, 40–70 min). The evolution of the transmitted light intensity in the blend exhibits two interesting features (Figure 3c). One is that the kinetics of the blend is intermediate between the two neat materials. For example, the crystallization of the blend at 240 °C completes at about 500 s, while it takes about 100 s for PEEK and 4000 s for PEKK(30/70) to complete. Second is that a two-step growth of the intensity profile is observed at all temperatures below 270 °C. In this process, a sharp increase in intensity is seen initially, followed by a slow rise. The initial rapid increase probably represents the crystallization of PEEK, and the later slow growth represents the crystallization of PEKK (30/70). This observation along with the finding of one speherulite morphology by optical microscopy indicates that in the blend, the PEEK spherulites are formed first, which

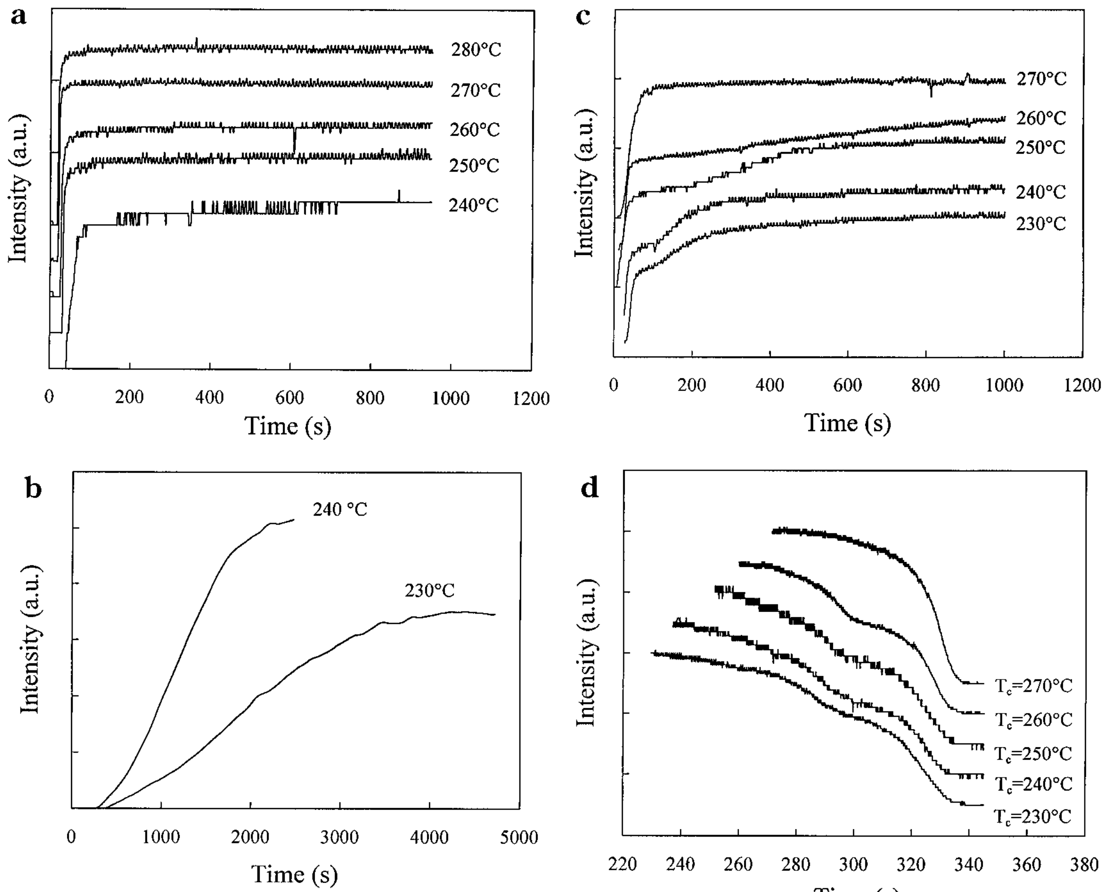

Figure 3. Transmitted light intensity of PEEK, PEKK(30/70), and the blend during isothermal crystallization of (a) PEEK, (b) PEKK(30/70), and (c) the PEEK/PEKK(30/70) blend and (d) during subsequent melting of the blend. All intensity profiles were vertically shifted with each other for clarity.

defines the overall morphological skeleton, and the PEKK(30/70) crystals are formed later within these spherulites.

Transmitted polarized light intensity profiles of the blend samples (crystallized at different temperatures) during subsequent melting are shown in Figure 3d. The heating rate of this experiment is 5 °C/min. It is seen that all intensities decrease as the temperature increases. In agreement with the observation during isothermal crystallization, a two-step intensity change is also seen in all samples precrystallized at temperatures from 230 to 270 °C. The onset of the two step changes is between 290 and 310 °C, which corresponds to the melting of PEKK(30/70). It is interesting to see that with the increase of precrystallization temperature, the onset temperature moves to a higher value and the magnitude of the first intensity drop also increases. This suggests the perfection of PEKK(30/70) crystals. From the optical microscopy, it is found that after the first intensity drop, the overall spherulite appearance remains the same but with a lessened birefringent strength. This is consistent with the argument that the two components (PEEK and PEKK(30/70)) are crystallized into two microstructures within the spherulites defined by PEEK. At temperatures above 330 °C, all intensities diminish to a negligible value, indicating the complete melting of the PEEK crystals.

Time-Resolved SAXS Results. The synchrotron SAXS technique was used to study the lamellar structures and their evolution of PEEK, PEKK, and the blend. Several lamellar variables have been extracted from the SAXS data using the correlation function method (eq 2). These variables include the thickness of lamellae l_c, the thickness of the amorphous layer l_a, the periodicity of the lamellar stacks (the long period $L = l_c + l_a$), and the invariant Q. As stated earlier, we have used a two-phase model proposed by Strobl and Schneider[35] for the data analysis. From eq 2, we obtain two thickness values for the phases l_1 and l_2 but cannot determine which one represents l_c or l_a. For the same reason cited by the authors in another paper,[36] we assign the higher value as the thickness of the lamellae and the smaller one as the thickness of the amorphous layers.

PEEK. Figure 4a shows the changes in L, l_c, and l_a during isothermal crystallization of PEEK at two temperatures (260 and 280 °C). It is seen that both L and l_c decrease with time, which is consistent with results observed previously.[15-17] The final values of the dimensions of the lamellar stacks of PEEK are $L = 135$ Å, $l_c = 88$ Å, and $l_a = 47$ Å for $T_c = 260$ °C and 142, 92, and 50 Å, respectively, for $T_c = 280$ °C. Both of these values (L and l_c) are found to increase with crystallization temperature T_c, which is expected from the thermodynamics consideration. Figure 4b shows the plots of L, l_c, and l_a against temperature during melting. The thermal history of the sample is as follows. After isothermal crystallization at 280 °C for 15 min, the sample was heated immediately at a rate of 5 °C/min. The data collecting time used was 27 s per scan (the temperature interval between adjacent scans was thus about 2.25 deg). It is seen that both L and l_c increase with temperature almost in a reversed fashion, as seen from the crystallization. However, it is interesting to note that the value of l_a remains almost constant. The initial increases of L and l_c are very small (below 300 °C), which are attributed to the effect of thermal expansion. The later increases (above 300 °C) are quite significant, which are attributed to the melting of thinner lamellae.

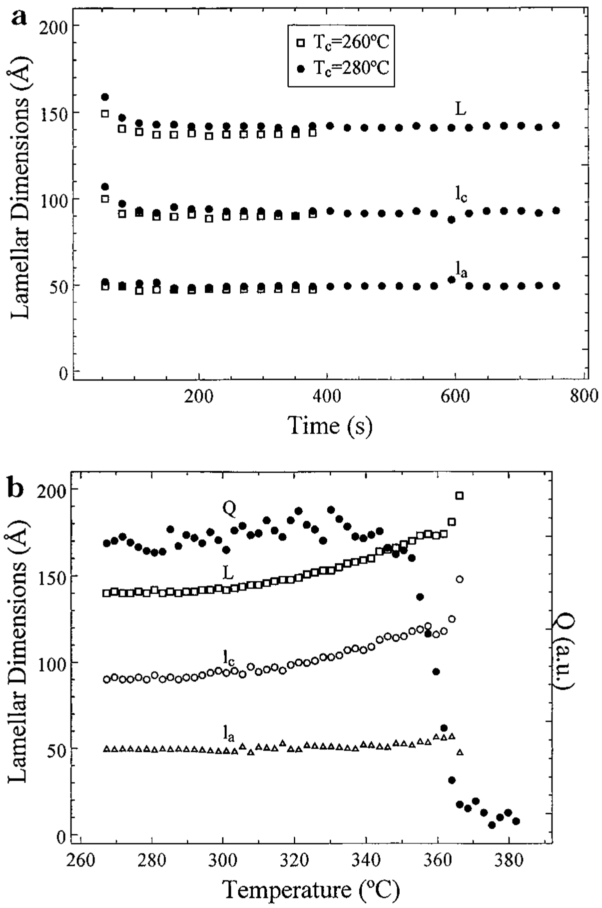

Figure 4. Lamellar dimensions (L, l_c, and l_a) of PEEK lamellar structure: (a) during (a) isothermal crystallization at 260 and 280 °C; (b) during melting at a 5 °C/min heating rate.

Table 1. Lamellar-Level Dimension of PEEK(30/70)

T_c	L, Å	l_c, Å	l_a, Å
240 °C	152	120	32
260 °C	174	151	23

PEKK(30/70). Since the crystallization kinetics of PEKK(30/70) is very slow, it is noneconomical to run the real time measurement using synchrotron radiations. PEKK(30/70) specimens were thus precrystallized off the beam line first and then characterized by synchrotron SAXS at the same crystallization temperature. The L, l_c, and l_a dimensions of PEKK(30/70), extracted from the correlation function, are listed in Table 1. The samples used were precrystallized at 240 °C for 20 h and 260 °C for 10 h, respectively.

It is seen that both L and l_c of PEKK(30/70) at 260 °C are higher than those at 240 °C (l_a shows an opposite trend). The higher value of lamellar thickness by increasing crystallization temperature is expected. However, this will not be the case if we assign the values of l_c and l_a inversely. Results in Table 1 thus confirm that the correct assignment of l_c and l_a has been made. Comparing the data in Table 1 with those in Figure 4, it is seen that the PEKK(30/70) lamellae have a larger long period and lamellar thickness but smaller amorphous layers than PEEK crystallized at the same temperatures. This is reasonable, since the equilibrium melting temperature of PEEK is much higher (about 90 °C) than PEKK(30/70) and the degree of undercooling

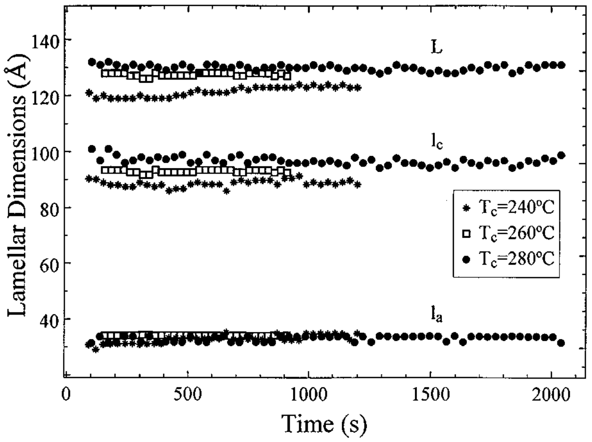

Figure 5. Lamellar dimensions (L, l_c, and l_a) of the PEEK/PEKK(30/70) blend during isothermal crystallization at 240, 260, and 280 °C.

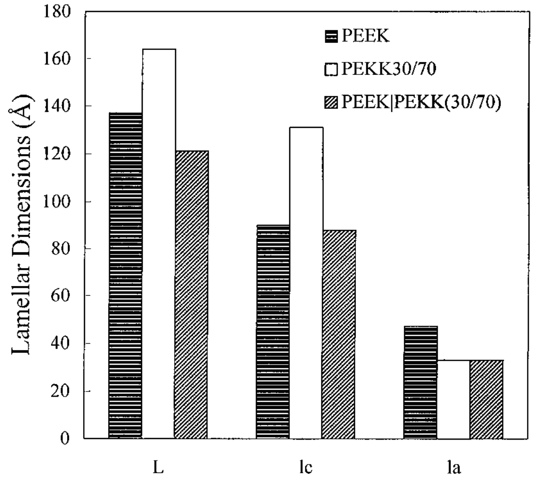

Figure 6. Comparison of final lamellar dimensions of PEEK, PEKK(30/70), and the blend crystallized at 260 °C.

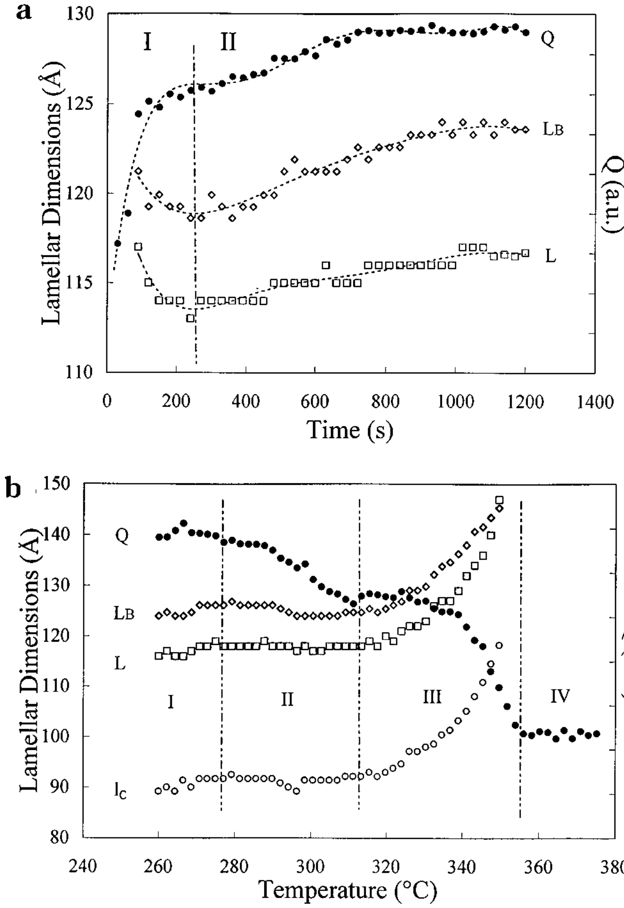

Figure 7. Changes in lamellar dimensions (L and l_c) and invariant Q of the PEEK/PEKK(30/70) blend during (a) isothermal crystallization at 260 °C and (b) the subsequent melting at 5 °C/min.

for PEKK(30/70) at the same crystallizing temperature is much smaller, resulting in a larger crystal thickness.

PEEK/PEKK(30/70) Blend. SAXS measurements were carried out for the blend during isothermal crystallization at different temperatures. Results are shown in Figure 5. Both values of L and l_c are seen to increase with crystallization temperature as expected, while the change in l_a is very small and independent of T_c. This again indicates that our assignment of l_c and l_a is correct. Now we turn our attention to the comparison of lamellar dimensions among PEEK, PEKK(30/70), and the blend. Figure 6 summarizes the final values of L, l_c, and l_a at a crystallization temperature of 260 °C. It is seen that both values of L and l_c of the blend are less than those of the neat materials, but very close to PEEK. This suggests that the faster crystallizing component PEEK dominates the microstructure morphology of the blend.

The detailed analysis of L in Figure 6 shows an interesting feature. This feature is illustrated in greater detail in Figure 7a, where two types of long periods (L and L_B) and the invariant are shown for isothermal crystallization at 260 °C (l_c shows an identical trend but l_a stays almost constant, both values are not included here). We have divided this figure into two stages (marked by the dotted line) to ease the discussion. It is seen that at stage I, both long periods decrease with time; whereas at stage II, both values increase. The corresponding invariant Q also exhibits a two-stage behavior: at stage I, the value increases at a rapid rate; at stage II, the increase slows down and gradually approaches a constant value. Note that the change of Q at 260 °C agrees well with that of the transmitted light intensity at the same temperature (Figure 3c). As discussed earlier, in the cases of isothermal crystallization of the neat polymers, both L and l_c decrease with time and Q shows only the stage I behavior. The unusual two-step change of L, l_c, and Q in Figure 7a indicates that two kinds of lamellar structures (PEEK and PEKK(30/70)) are formed separately during isothermal crystallization of the blend. The initial stage I is dominated by PEEK where its lamellar thickness is smaller and the later stage II is dominated by PEKK(30/70) where its lamellar thickness is larger (Figure 6), resulting in an increase of the average lamellar thickness.

SAXS measurement during subsequent melting of the blend was also performed immediately after the crystallization, and results are shown in Figure 7b. The thermal history of the sample is as such. After being held at 260 °C for 1200 s, the sample was heated to 380 °C at a rate of 5 °C/min. Changes in L, l_c, and Q during this measurement are plotted in Figure 7b. We have divided this figure into four stages for discussion. At stage I (260−285 °C), both L and l_c are seen to increase slightly with temperature, while Q shows a small decrease. This stage is probably due to the simple thermal expansion. At stage II (285−310 °C), L and l_c begin to decrease with temperature and Q decreases at a noticeable rate. This indicates that melting of the thicker PEKK(30/70) lamellae (lower melting point)

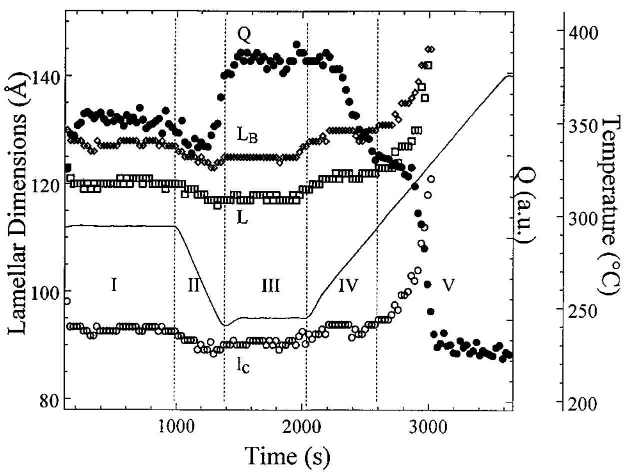

Figure 8. Lamellar dimensions (L and l_c) and invariant Q of the PEEK/PEKK(30/70) blend during stepwise isothermal crystallization and the subsequent melting measurements. The solid line represents the temperature profile.

occurs. Thus the net change in L and l_c in this stage is a result of the competition between the thermal expansion (which increases L and l_c) and the melting of the PEKK lamellae (which decreases the observed L and l_c). At stage III (310−350 °C), the rate of increase in L and l_c starts to escalate and the decrease in Q becomes quite significant. This stage represents the melting of the PEEK lamellae. The changes in L, l_c, and Q in this stage were similar to those observed during the melting of neat PEEK (Figure 4c). Stage IV represents the complete molten state.

We have additionally carried out a stepwise crystallization and subsequent heating for the blend to investigate the thermal effects of higher complication. The thermal profile imposed is as follows. The sample was first melted at 400 °C for 5 min and then rapidly transferred to the isothermal chamber at 300 °C for SAXS measurements. After the sample was crystallized for 15 min, it was cooled to 250 °C for 10 min for subsequent annealing. After this, the sample was immediately heated to 380 °C at a rate of 5 °C/min. This temperature profile is shown in Figure 8, along with the values of L, l_c, and Q. The average value of l_a was approximately 35 Å and virtually unchanged throughout the whole process; thus it is not included here. We have divided Figure 8 into five stages for discussion. Stage I represents the isothermal crystallization of the sample at 300 °C. Initially, Q increases rapidly and reaches its maximum at about 200 s, and the corresponding L and l_c decrease with time but soon level off. Since the temperature in this stage was only about 5 deg below the equilibrium melting temperature of PEKK(30/70), the undercooling is too small for PEKK(30/70) to crystallize. Consequently, we believe that only PEEK crystals are formed in this stage. Note that the final values of L and l_c in this stage are about 127 and 92 Å, which are less than those of pure PEEK crystallized isothermally at 280 °C. This is because the crystallization of the blend at this temperature is complete at about 400 s, which is longer than those of PEEK at this temperature.

Stage II in Figure 8 represents the cooling from 300 to 250 °C. Within this stage, all values of L and l_c decrease rapidly with time, where Q shows an initial decrease and then a subsequent increase. The initial decrease in Q can be explained by the effect of thermal contraction, and the later increase is due to the subsequent crystallization of PEEK by increasing the undercooling. Stage III represents the isothermal crystallization process at 250 °C. The behavior in this stage is somewhat similar to that in stage I; however, slight increases of L and l_c are seen at the end. The increases in L and l_c suggest that the thicker PEKK(30/70) lamellae are formed. Stage IV represents the heating of the sample between 250 and 300 °C. In this stage, L and l_c initially increase and then level off. The increase can be explained by the thermal expansion, but the level off indicates the melting of the thicker PEKK(30/70) lamellae. The rapid decrease in Q is consistent with the behavior of melting in this region. Stage V represents the melting of the residual PEEK lamellae. Again, the melting behavior in this region is similar to that of the melting of neat PEEK; i.e., L and l_c increase rapidly with temperature and Q rapidly diminishes to a negligible level.

Discussion

It is apparent that the presence of PEKK(30/70) significantly slows down the crystallization of PEEK, and two types of lamellar structures coexist within the spherulites defined by PEEK. Some of these observations are discussed with more detail in this section.

As noted from DSC (Figure 1) and transmitted light intensity (Figure 3) results, PEEK has faster crystallization kinetics (about 3 orders of magnitude) than PEKK(30/70). But the two interesting features in Figure 1 [(1) at temperatures above 280 °C and below 200 °C, the crystallization kinetics of the blend closely tracks that of pure PEEK, and (2) within the temperature region of 220−260 °C, the crystallization kinetics of the blend becomes intermediate between the two neat materials] deserve more explanation. The behavior in (1) is expected, since the crystallization rate of PEKK(30/70) in these temperature regions is so slow that no crystallization of PEKK(30/70) should occur within the experimental time, which leads to a PEEK dominating behavior. The apparent intermediate kinetics of the blend in (2) is probably due to two separate crystallization processes of similar crystallization rates. One process is the crystallization of PEEK, retarded by the interdiffusion between PEEK and PEKK(30/70). Since PEKK(30/70) is more flexible (higher keto and 1,3 linkages) than PEEK, its lower diffusivity thus can considerably slow down the kinetics of PEEK. Another process is the crystallization of PEKK(30/70), somehow accelerated by the presence of the PEEK crystals (probably the result of the change of local strain in the PEKK(30/70) melt). The increase of the PEKK(30/70) kinetics is not due to the effect of epitaxy between PEKK(30/70) and PEEK crystals, as from the observations of lamellar changes during crystallization and melting (Figures 7 and 8). This is explained below.

From transmitted light intensity and SAXS invariant results, we conclude that two crystal structures are formed during isothermal crystallization of the blend, as seen by the two-step growth behavior during crystallization (Figures 3c and 7a) and the reverse behavior during subsequent melting (Figures 3d, 7b, and 8). The onset of the two steps is indicative of the time when the change of the second structure (PEKK(30/70)) begins. From the profiles of the lamellar dimensions (Figures 7 and 8), we can further conclude that there is no cocrystallization or epitaxial growth between the PEEK and PEKK(30/70) crystals. This is because, if any of this process prevails, there should be no change of the long period during isothermal crystallization (although l_c should increase and l_a should decrease). This disagrees with our finding that the long period first decreases with time and then increases in the blend when PEKK(30/70) begins to crystallize (Figure 7a). The observation during melting reveals a similar story. First we find that the long period decreases (Figure 7b, stage II) when PEKK(30/70) starts to melt. This contradicts our expectation that the long period should remain constant when PEKK(30/70) melts, if it cocrystallizes or forms epitaxial structures with PEEK. Second, the value of l_a was found to stay almost constant throughout the melting process when PEKK(30/70) melts, rather than a sharp increase as cocrystallization occurs.

The only possible morphological model, consistent with our results, is that PEEK crystallizes first, forming spherulite morphology. PEKK(30/70) crystallizes later in an infilling fashion within these PEEK spherulites. The two components form separate lamellar stacks with different long periods and lamellar thicknesses. In this case, the decrease of L and l_c between 285 and 310 °C during heating (Figure 7b, stage II), is due to the melting of the thicker PEKK(30/70) stacks; the increase of L and l_c during isothermal crystallization (Figure 7a, stage II), is due to the formation of thicker PEKK(30/70) lamellae. This model thus suggests the complete rejection of PEKK(30/70) molecules in PEEK lamellar stacks. However, the scale of the phase separation induced by PEEK crystallization must be much smaller than that of the PEEK spherulites. This is because no separate PEKK(30/70) speherulite can be observed in the blend.

Conclusions

Two major conclusions have been made from the present work. (1) The crystallization kinetics of neat PEEK and PEKK(30/70) and their blend have been studied. Results indicate that PEKK(30/70) retards the kinetics of PEEK probably due to the interdiffusion process of the two components. In contrast, PEEK crystals are found to enhance the crystallization rate of PEKK(30/70), which is probably not by the effect of epitaxial growth but due to the change of the local strain in the residual PEKK(30/70) melt. (2) A two-step behavior has been observed during crystallization and subsequent melting processes. Our results exclude the possibility of cocrystallization but indicate the formation of two separate lamellar stacks (PEEK and PEKK(30/70)) within the spherulites of PEEK. The components of PEKK(30/70) are probably rejected in the region of the PEEK lamellar stacks, and crystallized later in an infilling fashion in the crystalline frame work defined by PEEK.

Acknowledgment. The authors wish to thank R. J. Trotman of DuPont and Mr. Fengji Yeh of SUNY at Stony Brook for their excellent technical assistance. We gratefully acknowledge the help of our colleagues at the Pattern Formation Research Group at the University of Delaware. This work was partially supported by the National Science Foundation, under grant DMR 9115308, and by E. I. du Pont de Nemours and Co.

References and Notes

(1) Blundell, D. J.; Osborn, B. N. *Polymer* **1983**, *24*, 953.
(2) Velisaris, C.; Seferis, J. *Polym. Eng. Sci.* **1986**, *26* (22), 1574.
(3) Pratt, J. F.; Krueger, W. H.; Chang, I. Y. *SAMPE Int. Symp.* **1989**, *34*, 2229.
(4) Harris, J. E.; Robeson, L. M. *J. Appl. Polym. Sci.* **1988**, *35*, 1877.
(5) Chang, I. Y. *SAMPE Q.* **1988**, *19*, 29.
(6) Gardner, K. H.; Hsiao, B. S.; Matheson, R. R., Jr; Wood, B. A. *Polymer* **1992**, *33*, 2483.
(7) Abraham, R. J.; Haworth, I. S. *Polymer* **1991**, *32*, 121.
(8) Jog, J. P.; Nadkarni, V. M. *J. Appl. Polym. Sci.* **1986**, *32*, 3317.
(9) Dawson, P. C.; Blundell, D. J. *Polymer* **1980**, *21*, 577.
(10) Hay, J. N.; Langford, J. I.; Lloyd, J. R. *Polymer* **1989**, *30*, 489.
(11) Hsiao, B. S.; Gardner, K. H.; Wu, D. Q.; Chu, B. *Polymer* **1993**, *34*, 3896.
(12) Bassett, D. C.; Olley, R. H.; Al Raheil, A. M. *Polymer* **1988**, *29*, 1745.
(13) Marand, H.; Prasad, A. *Macromolecules* **1992**, *25*, 1731.
(14) Hudson, S. D.; Davis, D. D.; Lovinger, A. J. *Macromolecules* **1992**, *25*, 1759.
(15) Wang, J.; Alvarez, M.; Zhang, W.; Wu, Z.; Li, Y.; Chu, B. *Macromolecules* **1992**, *25*, 6943.
(16) Hsiao, B. S.; Gardner, K. H.; Wu, D. Q.; Chu, B. *Polymer* **1993**, *34*, 4003.
(17) Kråger, K. N.; Zachmann, H. G. *Macromolecules* **1993**, *26*, 5202.
(18) Verma, R. K.; Kander, R. G.; Velikov, V.; Marand, H.; Hsiao, B. S.; Chu, B. *Bull. Am. Phys. Soc.* **1994**, *39*, 109.
(19) Cebe, P.; Hong, S. D. *Polymer* **1986**, *27*, 1183.
(20) Zhang, Z.; Zeng, H. *Polymer* **1993**, *34*, 4023.
(21) Hsiao, B. S.; Chang, I. Y.; Saue, B. B. *Polymer* **1991**, *32*, 2799.
(22) Damman, P.; Fougnies, C.; Moulin, J. F.; Dosiere, M. *Macromolecules* **1994**, *27*, 1582.
(23) Jonas, A.; Legras, R. *Polymer* **1991**, *32*, 2691.
(24) Kumar, S.; Anderson, D. P.; Adams, W. W. *Polymer* **1986**, *27*, 329.
(25) Hay, J. N.; Kemmish, D. J.; Langford, J. I.; Rae, A. I. M. *Polymer* **1984**, *29*, 175.
(26) Lattimer, M. P.; Hobbs, J. K.; Hill, M. J.; Barham, P. J. *Polymer* **1992**, *33*, 3971.
(27) Hsiao, B. S.; Gardner, K. H.; Cheng, S. Z. D. *J. Polym. Sci., Polym. Phys. Ed.* **1994**, *32*, 2585.
(28) Konnecke, K. *J. Macromol. Sci., Phys.* **1994**, *B33* (1), 37.
(29) Ho, R. M.; Cheng, S. Z. D.; Hsiao, B. S.; Gardner, K. H. *Macromolecules* **1994**, *27*, 2136, 5787.
(30) Ho, R. M.; Cheng, S. Z. D.; Hsiao, B. S.; Gardner, K. H. *Macromolecules* **1995**, *28*, 1938, 8855.
(31) Hsiao, B. S.; Gardner, K. H.; Schultz, J. M.; Wang, W. *Conference Proceedings of ANTEC '93*, New Orleans, May 9−13, 1993; 1993; p 1004.
(32) Chu, B.; Wu, D. Q.; Howard, R. *Rev. Sci. Instrum.* **1989**, *60*, 3224.
(33) Song, H. H.; Stein, R. S.; Ree, M.; Phillips, J. C.; LeGrand, A.; Chu, B. *Macromolecules* **1988**, *21*, 1180.
(34) Vonk, C. G. *J. Appl. Crystallogr.* **1973**, *6*, 81.
(35) Strobl, G. R.; Schneider, M. *J. Polym. Sci., Polym. Phys. Ed.* **1980**, *18*, 1343.
(36) Wang, W.; Schultz, J. M.; Hsiao, B. S. *J. Polym. Sci., Polym. Phys. Ed.* **1996**, *34*, 3095.
(37) Wang, W.; Schultz, J. M.; Hsiao, B. S. To be submitted for publication.

MA970092L